VOL. 14, NO. 6, MARCH 2019 ISSN 1819-6608
ARPN Journal of Engineering and Applied Sciences

www.arpnjournals.com

COMPARISON OF 2D AND 3D FINITE ELEMENT STRUCTURAL ANALYSIS OF FOUNDATION SLAB ON ELASTIC HALF-SPACE

Jiri Koktan, Radim Cajka and Jiri Brozovsky
Faculty of Civil Engineering, VŠB – Technical University of Ostrava, Faculty of Civil Engineering, Ludvíka Podéště, Ostrava, Czech Republic
E-Mail: jiri.koktan@vsb.cz

ABSTRACT

Structural analysis of interaction of foundation slab with subsoil represented by elastic half space can be performed by various numerical methods. Verification of 2D simplified FEA approach incorporating numerical integration of the Boussinesq solution is emphasized in this paper by direct comparison with 3D FEA, which uses semi-infinite elements. Both methods were used to solve two numerical examples and the result are presented and compared in this study. Paper also includes discussion of capabilities of both approaches with their advantages and disadvantages.

Keywords: foundation slab, subsoil interaction, FEA, elastic half-space, boussinesq, infinite boundary, numerical integration.

INTRODUCTION

The soil-structure interaction problem is one of the most common tasks among civil engineering computations. There are numerous approaches available [1], [2], [3]. The Finite Element Method [4] is usually used as a tool for computations.

However, the most common approach is to use 2D plate elements with the surface Winkler foundation model (Figure-1) which introduces subsoil effects in the vertical direction only. However, it is used today even for analysis of important structures, see [5] for its use in the process of assessment of a part of nuclear power plant or the paper [6] for an example of an analysis of tanks with fluids on the Winkler foundation.

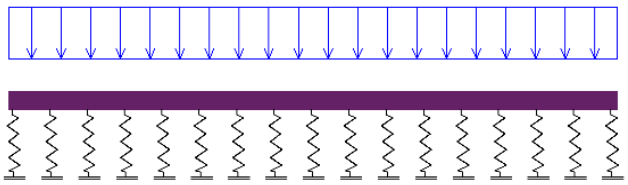

Figure-1. Winkler model for soil-structure interaction.

More complex approaches often model the subsoil with use of an elastic or in-elastic half-space [3], [7]. It makes possible to introduce many effects that can make the model very close to an actual behaviour of subsoil. The main disadvantage of such approach is that it results in solutions of large systems of linear or non-linear equations. The numbers of unknowns are usually in order of millions for 3D computations.

There are solution methods available for such large problems. They are often based on parallel solution [8] of the problem, which introduces further complexity to the model. For effective solution Domain decomposition methods are often used here, for example the FETI method [9].

It is possible to use analytical or numerical solution of parts of half-space as a basis for improvements of the Winkler model. One of such approaches was introduced by Čajka and used for various problems [10]. The results were verified by comparison with various experimental data, both obtained by the author of the method [11] and obtained by others [12], [13], [14]. However, this approach was implemented in late 1990s and the used software tools allowed verifying its behaviour only on relatively small problems. Thus, the main aim of the works discussed here is a modern implementation of the method which allows analysing problems of arbitrary size and a direct comparison with different method to verify this approach.

The main advantage of the method is its possibility of incorporation of more complex soil models with no requirements for homogeneity in any direction because the method allows to incorporate also more complex analytical parts (not only the Boussinesq solution). For sake of simplicity in this text, it will be assumed that the Winkler-type subsoil model is used for solving slabs on elastic homogenous half-space.

DESCRIPTION OF METHOD

The above-mentioned method uses features of isoparametric finite elements and their integration procedures [15]. The elastic half-space properties are based on the well-known Boussinesq analytical formulae [10]. For the purpose of the solution, the equation for the vertical stress σ_z can be written in the form:

$$\sigma_z = \frac{F}{2\pi} \cdot \frac{3 \cdot z^3}{r^5}, \tag{1}$$

where r, z are coordinates shown in the Figure-2 and F is a load in the form of vertical force.

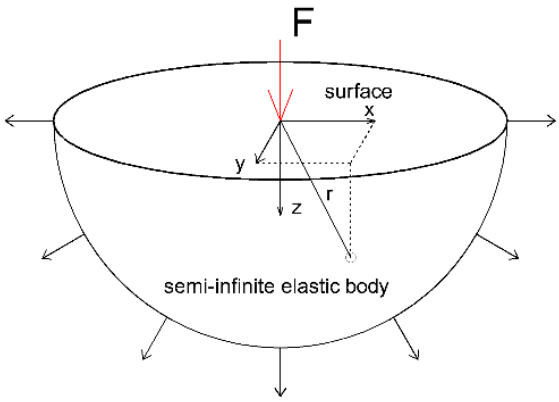

Figure-2. Elastic half-space model for Boussinesq solution.

The Equation (1) modified for constant pressure on rectangular area is often used in design standards and is suitable for analytical computations (for so-called engineering computations which do not require computer-based methods). For more complex cases it is necessary to work with formula which can incorporate general contacts stress p_z:

$$\sigma_z = \int_A \frac{p_z}{2\pi} \cdot \frac{3 \cdot z^3}{r^5} dA, \quad (2)$$

where A is area of solution (it can be area of a finite element or of its part belonging to an integration point). The actual use of the Equation (2) requires using numerical integration. The process of computation of stiffness matrices of isoparametric finite elements incorporates numerical integration (usually based on the Gauss formula) [15] and this procedure can also be utilized for computing of subsoil stiffness. For such purpose the Equation (2) should be replaced by its approximation:

$$\sigma_z = \sum_m \sum_n \frac{p_z(\xi,\eta)}{2\pi} \cdot \frac{3 \cdot z^3}{r^5} \Delta\xi \Delta\eta \det(\mathbf{J}), \quad (3)$$

where ζ, η are coordinates of coordinate system used for integration (natural coordinates) and the J is the Jacobian of transformation which is used for transformation from natural coordinates to real coordinates of the problem [15], [4]. The transformation and numerical integration are illustrated in Figure 3 for a 4-node isoparametric plate element.

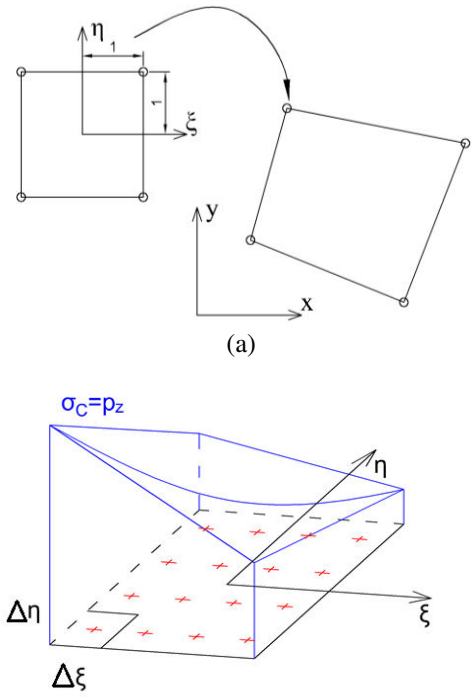

Figure-3. Transformation from natural coordinate system to real coordinate (a) and numerical integration in natural coordinate system of a 4-node element region (b).

Earlier implementation of the method used the same Gauss integration scheme as for the integration of element stiffness matrix [10]. The new implementation uses two-dimensional rectangular rule for calculating the vertical stress and deformation of the subsoil. The sample points are marked with red crosses in Figure-3. Considering that the integrand in equation (2) is not a polynomial function and that the integrated region (surface loaded by contact pressure) is separated into more elements there is no benefit in using Gauss integration scheme separately over elements.

Vertical stress and strain are decreasing with increasing depth z and go to zero in infinite depth. In design standards the active depth is usually reduced to a layer of finite thickness. Originally the procedure introduced by Čajka computes the subsidence of subsoil by numerical integration of formula:

$$s = \int_0^{z_a} \frac{1}{E_{oed}} (\sigma_z - m \cdot \sigma_{or}) dz, \quad (4)$$

where E_{oed} is oedometric modulus, z_a is active depth, m is structural strength constant and σ_{or} is original geostatic stress. Formula (4) introduces a reduction of vertical deformation which is based on experimental data but is not connected with the constitutive equations of elastic body. It is impossible to include same reduction of vertical deformations of the elastic half-space in general

purpose FEM software for structural analysis that works with three-dimensional volume elements. Thus, do not allow the direct comparison of the solution.

For the purpose of comparison and proof of concept of the procedure described below, formula (4) must be replaced by formula (5) which gives exact vertical deformation without any artificial reduction.

$$U_z = \int_A \frac{p_z}{2\pi} \frac{1+\nu}{E} \left(\frac{z^2}{r^3} + 2\frac{1-\nu}{r} \right) dA, \quad (5)$$

where E is Young modulus of the material and v is Poisson ratio. Equation (5) is derived from Boussinesq analytical formulae in the same way as equation (2) for vertical stress. Similarly, a numerical approximation (6) is used in the procedure of computing vertical deformation in every node of FE mesh.

$$U_z = \sum_m \sum_n \frac{p_z(\xi,\eta)}{2\pi} \frac{1+\nu}{E} \left(\frac{z^2}{r^3} + 2\frac{1-\nu}{r} \right) \Delta\xi\Delta\eta \det(\mathbf{J}), \quad (6)$$

The analysis of the soil-structure interaction problem must be done iteratively in several steps. For sake of simplicity, the text below will assume that the subsoil model includes only one parameter - a Winkler-style stiffness C in the vertical direction. Deformation and stiffness of the subsoil in horizontal directions will be neglected.

The procedure

a) Finite elements analysis of a slab structure with use of initial soil stiffness C. Resulting vertical deformation of the slab will be denoted as w to distinguish it from subsidence of the subsoil U_z.

b) Calculation of contact stresses $\sigma_{c,i}$ from vertical deformations w_i in every node of FE mesh:

$$\sigma_{c,i} = C_i \cdot w_i \quad (7)$$

c) Solution of subsidence U_z of elastic half-space caused by the calculated contact stress by numerical integration of analytical solution with use of the Equation (4) or (6) in the nodes.

d) Determination of new C_i parameters in every node of the structure:

$$C_i = \frac{\sigma_{c,i}}{U_{z,i}} \quad (8)$$

e) Finite elements analysis of structure with use of the new C_i parameters.

f) The steps 2. . . 5 should be repeated until the convergence is reached (the difference between U_z and w is insignificant).

In numerical examples, the iteration loop is controlled by following condition:

$$\frac{\|(\mathbf{u_i} - \mathbf{u_{i-1}})\|}{\|\mathbf{u_i}\|} < 1e^{-3}, \quad (9)$$

where $\mathbf{u_i}$ is vector of nodal deformations from i-th iteration cycle.

NUMERICAL EXAMPLES

To demonstrate the discussed model two simple examples are presented. The model discussed in this paper was implemented with use of the MATLAB software as a part of finite element code prepared by authors of this paper. A four-node and nine-node isoparametric shell finite elements have been used.

The code has a capability of changing status contact nonlinearity. After second step of the procedure contact stress is checked in every node. In case there is tension in any node the contact status is changed for this node and C_i stiffness parameter is significantly reduced. Step 2 is repeated until there is compression in every node of the plate structure that is in contact with subsoil. The behaviour of slab that tends to lift of the subsoil is illustrated in numerical example no. 2 which shows eccentrically loaded slab on relatively stiff subsoil.

Numerical example no.1 shows circular-shaped rotationally symmetrical slab which is relatively stiff in bending compared to the stiffness of the subsoil. Two load cases are discussed here. One for uniform distributed pressure and the other for load by concentrated force in the centre point.

Description of verification models

Both numerical examples were also analysed with use of general-purpose finite element software ANSYS Mechanical for structural analysis. A more complex 3D model that is shown in Figure-4 was created for the comparison and verification of described method.

The subsoil was modelled as elastic half-space. Meshed geometry of subsoil is a hemisphere with radius of 4 meters. The internal part within radius of 2 meters is meshed with ordinary isoparametric 20-node brick elements - SOLID186 (cyan elements in Figure-4). Outside this radius semi-infinite elements. - INFIN257 - are used to model infinite boundary [16] of the elastic half-space.

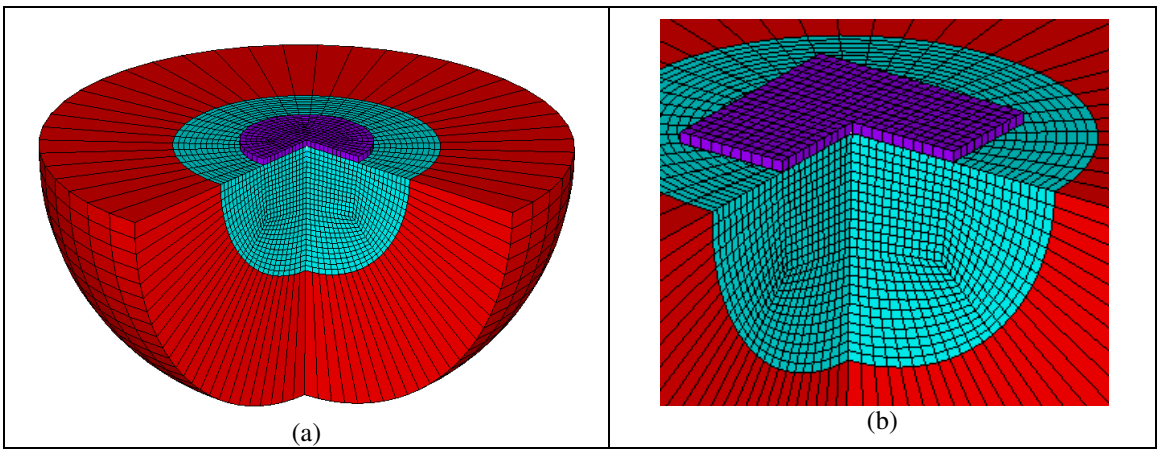

Figure-4. Three-dimensional verification model (¾ sector) - ANSYS. Circular slab (a) from example no. 1 and rectangular slab in detailed view from example no. 2 laid on hemisphere representing elastic half-space.

Definition of these elements is similar to isoparametric elements. They both use similar and compatible interpolation shape functions and they both use integration in natural coordinates system. The difference is in the transformation of the unit cube in natural coordinate system into real coordinate system. Mapping functions are used to project one side of the semi-infinite element into infinity. In this case, projection from one point that is located in the centre of the hemisphere is used. The red elements shown in Figure 4 are actually only halves of the semi-infinite elements. Nodes attached to the side that is projected into infinity are not shown. All degreases of freedom associated with these nodes are set to zero in element definition. Thus, they do not occur in resulting system of linear equations and there is no need to enter any additional boundary conditions to subsoil nodes. There are approximately 230000 additional equations associated with the subsoil compared to 8000 equations for the actual structure for this relatively small problem. Number of nodes in the slab structure is effectively the same in both MATLAB and ANSYS analysis.

Slabs are modelled with 8-node shell elements. - SHELL281 - in both examples. Slabs are connected to the subsoil using surface to surface contact pair TARGE170 - CONTA174. The contact between the slabs and foundation has standard behaviour with zero friction. Material properties and geometry of slabs is described below.

Numerical example 1

In first numerical example a circular shaped slab of a diameter of 2 metres on relatively soft subsoil was analysed. There are two load cases which are shown in Figure-5 (a). Both load cases are symmetrical with no eccentricity. This is an example of a slab that is entirely pushed into the subsoil and both contact surfaces don't tend to separate.

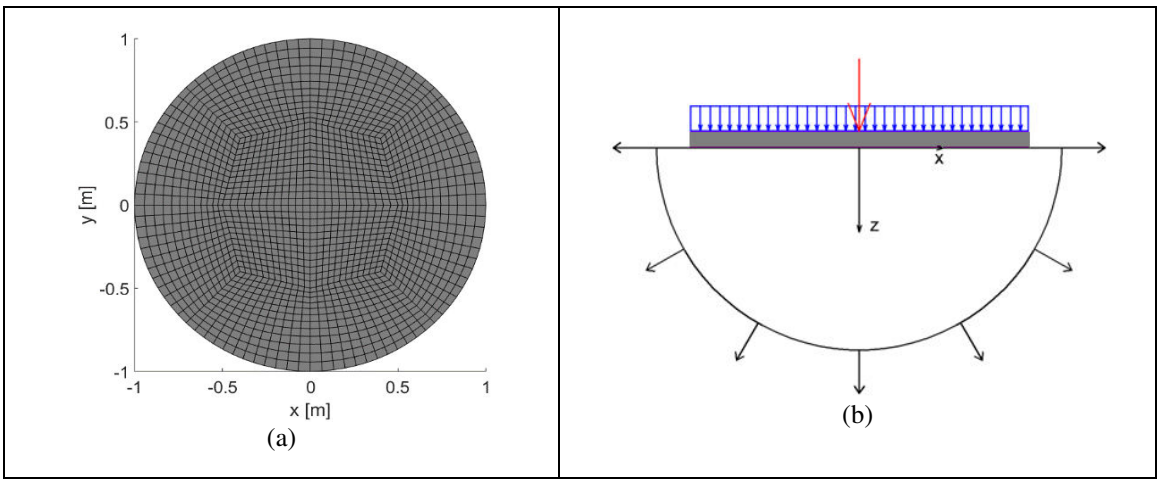

Figure-5. Geometry and FE mesh of circular slab from example 1 (a). Loading scheme of two load cases (concentrated force in the centre point and uniform pressure) (b).

The circular mesh was created by function in authors' code which uses a transformation of regular square meshes by quadratic interpolation functions.

In the first load case the slab was loaded by concentrated force of 3 MN in the centre point. In the

second load case the slab was loaded by uniform pressure of 1 MPa on the whole surface.

Both the slab and the subsoil are analysed with assumption of linear elastic behaviour. Material properties and other input values are following:

- Young's modulus of elasticity of the slab: E=30 GPa.
- Poisson ratio: v=0.2.
- Thickness of the slab: h=100 mm.
- Young's modulus of elasticity of the subsoil: E_{soil}=60 MPa.
- Poisson ratio: v_{soil}=0.35.

Both 4-node and 9-node elements were used in the analysis performed in MATLAB. The same total number of nodes and integration points were used to calculate subsidence of the subsoil for both types of elements (2 by 2 integration points per 4-node element and 4 by 4 integration points per 9-node element).

Results

In the first load case the solution converged after 8 iterations while in the second load case the solution converged after 12 iterations. The resulting deformation and contact pressure are drawn in radial cross-section (in the vertical plain y=0). In the graphs the axis x=0 is the axis of symmetry. Results from the analysis based on the method described above are labelled "SURFACE MODEL" and results from verification ANSYS analysis are labelled "ANSYS MODEL".

Figure-6 shows that the results from MATLAB analysis correspond with the ANSYS solution in both contact pressure and deformation. Graphs shows only negligible difference around the centre point where the concentrated force is applied.

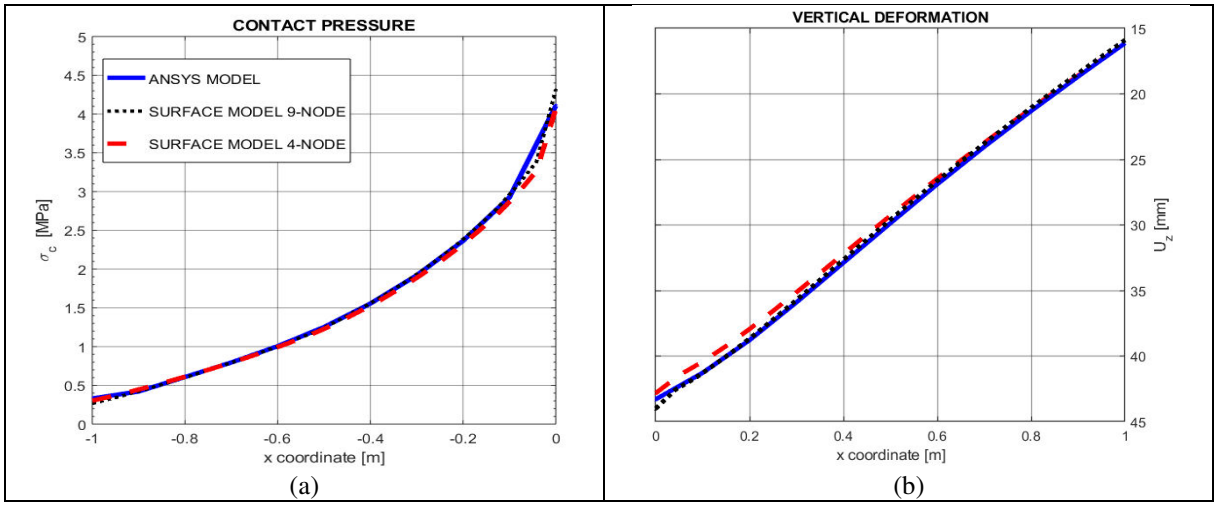

Figure-6. Loading case 1. Contact pressure (a) and vertical deformation of the subsoil (b) in radial cross-section.

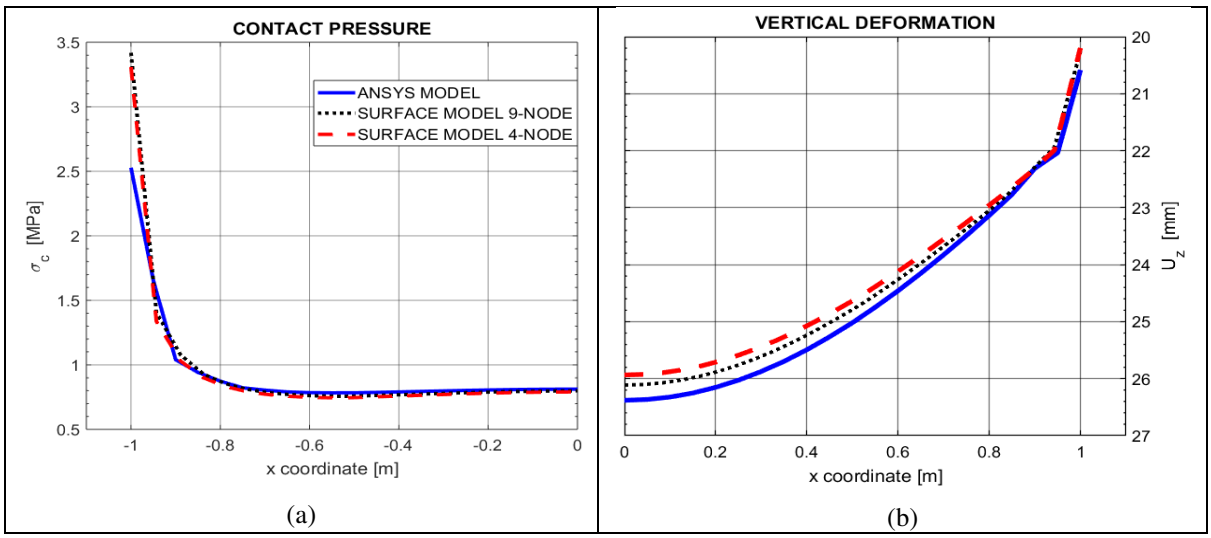

Figure-7. Loading case 2. Contact pressure (a) and vertical deformation of the subsoil (b) in radial cross-section.

Graph in the Figure-7 (a) shows a significant difference in contact stress near the edge of the slab. There is a large stress gradient near the edge as expected because the slab is stiff in bending compared to the soft subsoil. The difference would be even more significant if the FE mesh was finer. Stress results from numerical solution in this location are unreliable also in case of ANSYS analysis. On the other hand, this inaccuracy in stress peak has almost no effect on stress analysis of the slab and final subsidence of the foundation. In real foundation structure this stress peak is limited by exceeding the strength of the foundation soil that results in development of small zone of inelastic deformations near the edge of foundation slab.

During the procedure described above it causes inconsistent deformation of the slab and the subsoil which is shown in the Figure-8.

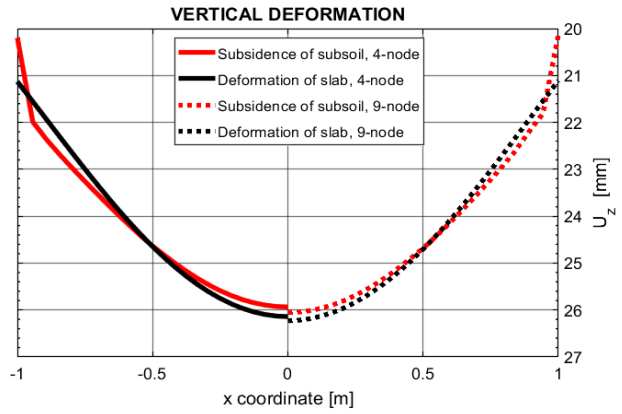

Figure-8. Vertical deformation of the slab and the subsoil in last iteration. Results from analysis using 4-node element on the left and 9-node element on the right.

It also affects convergence of the solution. To satisfy the convergence condition (9) it took 5 more iteration steps in case of uniform load than in case of concentrated load with no other change in the analysis. The comparison of convergence for both load cases is shown in the Figure-9 where values on the vertical axis corresponds with the left side of condition (9).

From comparison of 4-node and 9-node element solution it's obvious that using higher order element doesn't quite solve this issue. The number of iterations required to meet convergence criterium is the same even though the inconsistency in deformation is less noticeable in case of 9-node element.

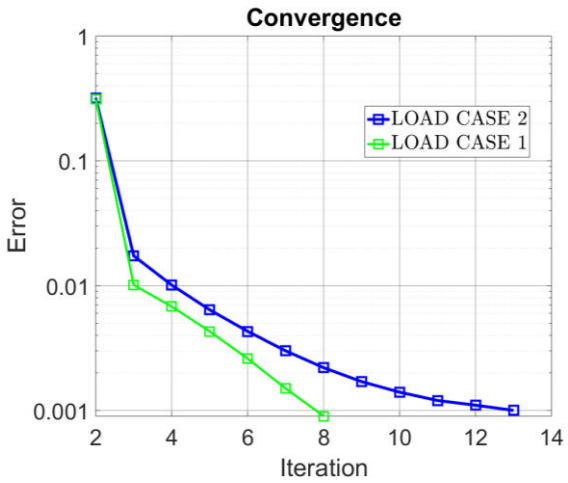

Figure-9. Vertical deformation of the slab and the subsoil in last iteration. Results from analysis using 4-node element on the left and 9-node element on the right.

Numerical example 2

Example number 2 shows a case of square slab that is loaded eccentrically. The load consists of vertical force F_z=4 MN and moments in two axes M_x=M_y=1MNm. This type of load causes that part of the slab tent to lift and separate from the subsoil. This would result in tension between the two surfaces if changing status nonlinearity wouldn't be incorporated. This example shows that the proposed method is capable of such nonlinear analysis.

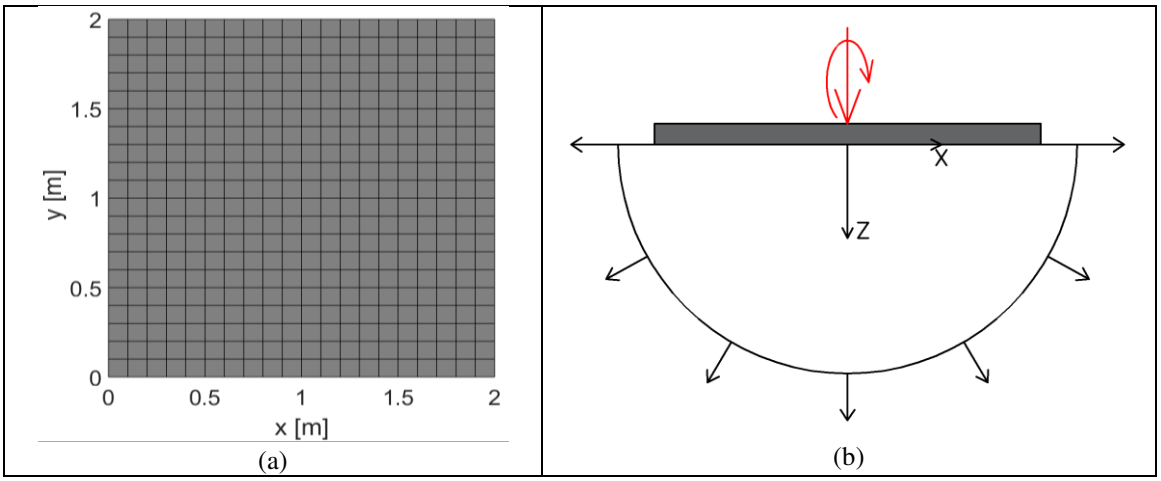

Figure-10. Geometry and FE mesh of the square slab from example 2(a). Loading scheme (eccentrically vertical force) (b).

The geometry is shown in the Figure-10 as well as loading scheme. Material properties of both the slab (including thickness) and the subsoil are the same as in example 1. The number of integration point used for calculation of subsoil deformation are again 4 by 4 points per element. Only 9-node quadratic element was used in analysis and the slab was meshed with 10 by 10 elements. This problem was also solved using ANSYS for verification of results.

Results

In the Figure-11 deformed FE meshes are shown from both MATLAB and ANSYS analysis. It is shown that the resulting deformations are almost identical. More detailed results are shown in the Figure-12 (a) where vertical deformation is plotted in the diagonal cross-section.

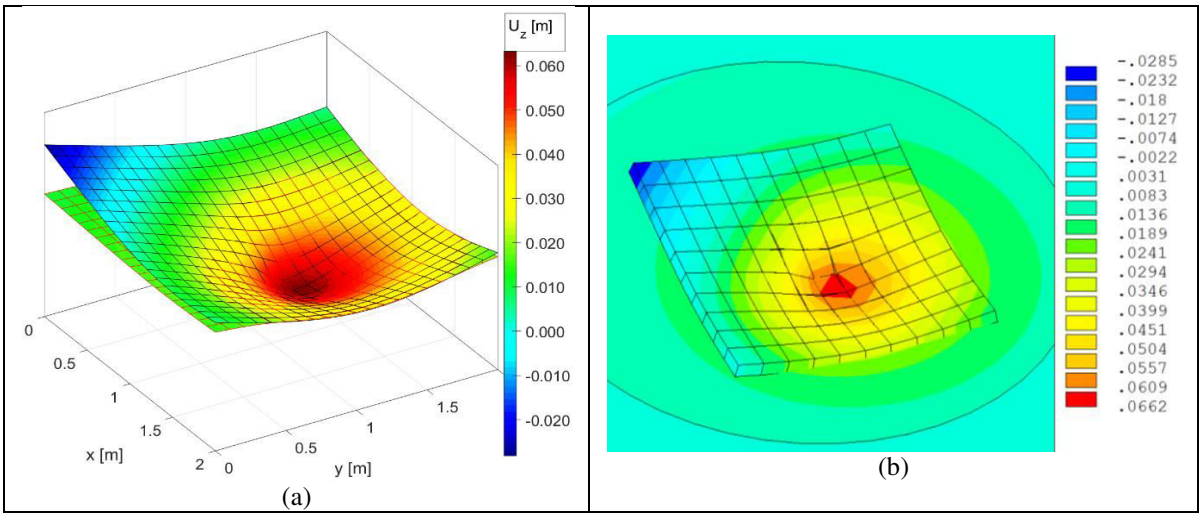

Figure-11. Vertical deformation contour plot of deformed model from MATLAB and ANSYS analysis.

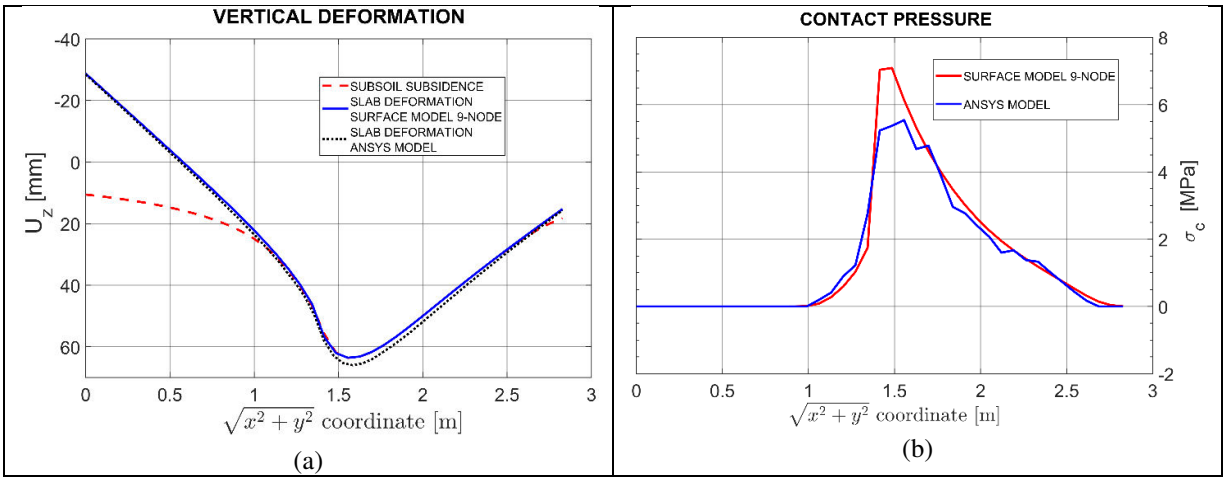

Figure-12. Results in diagonal cross-section. Vertical deformation of the subsoil and the slab (a). Contact pressure (b).

CONCLUSIONS

The proposed approach can provide results, which are comparable to results obtained by numerical computation on the 3D half-space model. The main advantages of the presented model are a much smaller size of problem in terms of unknowns (when compared with 3D half-space models) and the versatility in possible models of subsoil behaviour (there is no requirement of homogeneity of subsoil in any direction).

It has been verified that this approach gives correct results for arbitrary geometry and boundary conditions configuration by a direct comparison with results obtain by different method. Even in case of eccentric loading when part of the slab tents to lift from the subsoil.

It has been also verified that the method is scalable, and the results don't degrade with size of the problem. It wasn't possible to verify this fact with the original software implementation by Čajka because of the given constrains of problem size. The prepared software code is going to be used in further development of the method. The procedures for incorporation of layered subsoil are going to be implemented, for example.

ACKNOWLEDGEMENTS

This paper has been written with the financial support of the Ministry of Education, specifically by the Student Research Grant Competition of the Technical University of Ostrava under identification number SP2018/141.

REFERENCES

[1] Wang B., Zhou S. & Wang C. 2011. Settlement Calculation Method with Pile-Net Composite Foundation. ICCTP.

[2] X. Huang, X. Liang, M. Liang, M. Deng, A. Zhu, Y. Xu, Y. Li, and X. Wang. 2013. Experimental and theoretical studies on interaction of beam and slab for cast-in-situ reinforced concrete floor structure. Jianzhu Jiegou Xuebao/Journal of Building Structures. 34(5): 63-71.

[3] Zhou K., Wayne Chen W., Keer L. M., Ai X., Sawamiphakdi K., Glaws P. & Jane Wang Q. 2011. Multiple 3D inhomogeneous inclusions in a half space under contact loading. Mechanics of Materials. 43(8): 444-457.

[4] Zienkiewicz O. C., Zhu J. Z. & Taylor R. L. 2005. Finite Element Method: Its Basis and Fundamentals. Elsevier.

[5] Kralik J., Jendzelovsky N. 1993. Contact problem of reinforced-concrete girder and nonlinear Winkler foundation. International Conference Geomechanics.

[6] Kotrasova K., Grajciar I. & Kormanikova E. 2015. A case study on the seismic behavior of tanks considering soil-structure-fluid interaction. Journal of vibration engineering & technologies. 3(3): 315-330.

[7] Fabrikant V. I. & Sankar T. S. 1984. On contact problems in an inhomogeneous half-space. International Journal of Solids and Structures. 20(2): 159-166.

[8] Fialko S. 2015. Parallel direct solver for solving systems of linear equations resulting from finite element method on multi-core desktops and workstations. Computers & Mathematics with Applications. 70(12): 2968-2987.

[9] Farhat C. & Roux F.-X. 1991. A method of finite element tearing and interconnecting and its parallel solution algorithm. International Journal for Numerical Methods in Engineering. 32(6): 1205-1227.

[10] Čajka R. 2013. Analysis of Stress in Half-Space Using Jacobian of Transformation and Gauss Numerical Integration. Advanced Materials Research. 818: 178-186.

[11] Čajka R. 2014. Comparison of the Calculated and Experimentally Measured Values of Settlement and Stress State of Concrete Slab on Subsoil. Applied Mechanics and Materials. 501-504, 867-876.

[12] Zhao C. Y. 2011. Study on Bearing Capacity of Weaken Foundation by Field In-Situ Tests in Zhangjiajie-Huayuan Expressway. Contemporary Topics on Testing, Modeling, and Case Studies of Geomaterials, Pavements, and Tunnels.

[13] Zhang Z. M., Chen H. & Wu H. M. 2004. Research on stress and settlement of composite ground with soft base slab. Rock and Soil Mechanics. 25(3): 451-454.

[14] Alani A. M., Rizzuto J., Beckett D. & Aboutalebi M. 2014. Structural behaviour and deformation patterns in loaded plain concrete ground-supported slabs. Structural Concrete. 15(1): 81-93.

[15] Irons B. M. 1974. A technique for degenerating brick-type isoparametric elements using hierarchical midside nodes. International Journal for Numerical Methods in Engineering. 8(1): 203-209.

[16] Zienkiewicz O. C., Emson C. & Bettess P. 1983. A novel boundary infinite element. International Journal for Numerical Methods in Engineering. 19(3): 393-404.